Heliyon 10 (2024) e24103

Contents lists available at ScienceDirect

Heliyon

journal homepage: www.cell.com/heliyon

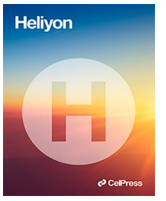

Research article

The lncRNA GAS5 upregulates ANXA2 to mediate the macrophage inflammatory response during atherosclerosis development☆

Yuzhou Xue [a,b], Yu Hu [b,h], Shikai Yu [c], Wenyan Zhu [d,f], Lin Liu [e], Minghao Luo [b], Suxin Luo [b], Jian Shen [b], Longxiang Huang [b], Jie Liu [c], Dingyi Lv [b], Wenming Zhang [a], Jingyu Wang [g], Xiang Li [b,*]

[a] *Department of Cardiology and Institute of Vascular Medicine, NHC Key Laboratory of Cardiovascular Molecular Biology and Regulatory Peptides, State Key Laboratory of Vascular Homeostasis and Remodeling, Peking University Beijing Key Laboratory of Cardiovascular Receptors Research, Peking University Third Hospital, Beijing, China*
[b] *Department of Cardiology, the First Affiliated Hospital of Chongqing Medical University, Chongqing, China*
[c] *Department of Cardiology, Shanghai Tenth People's Hospital, Tongji University School of Medicine, Shanghai, 200072, China*
[d] *Chongqing Engineering Research Center of Pharmaceutical Sciences, Chongqing Medical and Pharmaceutical College, Chongqing, 401331, China*
[e] *Department of Dermatology, the First Affiliated Hospital of Chongqing Medical University, Chongqing, China*
[f] *Department of Pharmacology, College of Pharmacy, Chongqing Medical University, Chongqing, 400016, China*
[g] *Renal Division Key Laboratory of Renal Disease Key Laboratory of Chronic Kidney Disease Prevention and Treatment (Peking University), Ministry of Education, Peking University First Hospital, Peking University Institute of Nephrology, Ministry of Health of China, Beijing, 100034, China*
[h] *Yongchuan Hospital of Chongqing Medical University, Chongqing, 402160, China*

ARTICLE INFO

Keywords:
Atherosclerosis
GAS5
ANXA2
Inflammatory response
Apoptosis
Macrophage

ABSTRACT

Inflammatory macrophages play a crucial role in atherosclerosis development. The long non-coding RNA growth arrest-specific 5 (GAS5) regulates THP-1 macrophage inflammation by sponging microRNAs. The purpose of this study was to investigate the regulatory mechanism of GAS5 in atherosclerosis development. GSE40231, GSE21545, and GSE28829 datasets from the Gene Expression Omnibus database were integrated after adjusting for batch effect. Differential analysis was performed on the integrated dataset and validated using the Genotype-Tissue Expression and GSE57691 datasets. Potential biological functions of GAS5 and annexin A2 (ANXA2) were identified using gene set enrichment analysis (GSEA). ssGSEA, CIBERSORTx, and ImmuCellAI algorithms were used to identify immune infiltration in plaque samples. GAS5 and ANXA2 expression levels in RAW264.7 cells treated with oxidized low-density lipoprotein (ox-LDL) were measured by qRT-PCR and Western blot. Small interfering and short hairpin RNA were used to silence GAS5 expression. Plasmids of ANXA2 were used to establish ANXA2 over-expression. Apoptosis and inflammatory markers in macrophages were detected by Western blot. Aortic samples from $APOE^{-/-}$ mice were collected to validate the expression of GAS5 and ANXA2. GAS5 expression was significantly increased during atherosclerosis. GAS5 expression was positively correlated with macrophage activation and ANXA2 expression in plaques. Furthermore, ANXA2 upregulation was also related to the activation of macrophage. GSEA indicated similar biological functions for GAS5 and ANXA2 in plaques. Moreover, *in vitro* experiments showed that both GAS5 and ANXA2 contributed to macrophage apoptosis and inflammation. Rescue assays

☆ Yuzhou Xue, Yu Hu, Shikai Yu contributed equally in this paper.

* Corresponding author. Department of Cardiology, The First Affiliated Hospital of Chongqing Medical University, No.1 Youyi Road, Yuzhong District, Chongqing, China.
E-mail addresses: lzd9288@163.com, lixiang@hospital.cqmu.edu.cn (X. Li).

https://doi.org/10.1016/j.heliyon.2024.e24103
Received 7 May 2023; Received in revised form 1 January 2024; Accepted 3 January 2024
Available online 4 January 2024

revealed that the inflammatory effects of GAS5 on macrophages were ANXA2-dependent. In vivo experiments confirmed the highly expression of Gas5 and Anxa2 in the plaque group. We identified the atherogenic roles of GAS5 and ANXA2 in the inflammatory response of macrophages. The inflammatory response in ox-LDL-treated macrophages was found to be mediated by GAS5-ANXA2 regulation, opening new avenues for atherosclerosis therapy.

1. Introduction

Atherosclerosis, mainly manifested as ischemic heart disease and ischemic stroke, is a leading cause of death worldwide, and its incidence has increased recently [1,2]. Vascular inflammation plays a central role in atherosclerosis and promotes plaque formation and instability [3,4]. With the development of single-cell sequencing technology, the phenotypic *trans*-differentiation of immune cells has been revealed [5,6]. Macrophage are classified into three subtypes: inflammatory, resident, and highly triggering receptor expressed on myeloid cells 2 (TREM2-high) [7,8]. Inflammatory macrophages enriched in cytokines and chemokines within the intima of the plaque are considered the main cause of lesion inflammation [9,10].

Long noncoding RNAs (lncRNAs) have emerged as key mechanistic regulators of gene expression and protein function in the pathogenesis of atherosclerosis [11,12]. Growth arrest–specific 5 (GAS5), a widely studied lncRNA, is abundant in macrophages and endothelial cells in plaques and may be involved in the development of atherosclerosis [13–15]. GAS5 regulates macrophage inflammation, apoptosis, and lipid accumulation by sponging micro-RNAs [16–18]. However, the mechanism by which GAS5 induces the *trans*-differentiation of macrophages into the inflammatory subtype has not been investigated. According to our previous study, GAS5 can directly bind to annexin A2 (ANXA2), which was identified using an RNA pull-down assay [19]. In the present study, we further investigated the correlation between GAS5 and ANXA2 expression in atherosclerosis. Based on various datasets, we found that GAS5 and its downstream target, ANXA2, are associated with the development of atherosclerosis and macrophage activation. Further experiments suggested that GAS5 could bind directly to ANXA2 and knockdown of both could reverse the inflammatory macrophage differentiation.

2. Materials and methods

2.1. Data source and preprocessing

Using the keywords “atherosclerosis” and “*Homo sapiens*”, datasets of plaque and normal tissue samples from the Gene Expression Omnibus (GEO) database (https://www.ncbi.nlm.nih.gov/geo/) were retrieved for analysis. The raw data (CEL files) of GSE40231 (n = 80), GSE21545 (n = 126), and GSE28829 (n = 29), tested on GPL570 platform, which is based on the Affymetrix Human GenomeU133 Plus 2.0 Array, were preprocessed and normalized using the RMA algorithm by affy package [20]. We then performed *ComBat* function to remove the batch effects among these three datasets, and a total of 235 samples were assembled into an integrated dataset using the sva R package [21]. Principal component analysis revealed that three datasets were appropriately integrated together after removing batch (Supplementary Figs. 1A–B). The Genotype-Tissue Expression (GTEx) database (https://gtexportal.org/) was downloaded, and plaque and normal sample datasets from coronary arteries were extracted according to the file “GTEx_Analysis_v8_Annotations_SampleAttributesDS.txt”. GTEx dataset (n = 432) and GSE57691 (n = 19 based on GPL10558) were used as validation datasets for differential expression of GAS5 and ANXA2. To further validate the differential expression of GAS5 and ANXA2 in macrophages treated with oxidized low-density lipoprotein (ox-LDL), GSE54039 (THP-1 macrophage treated with ox-LDL) (n = 6) tested on GPL13825 and GSE58913 (resident peritoneal macrophages treated with ox-LDL) (n = 6) tested on GPL17946 were enrolled in our study. The characteristics of all datasets analyzed in our study are summarized in Supplementary Table 1. The gene probes were aligned with the official gene symbol after log2 transformation and normalization. The median gene expression value was acquired if more than one probe matched a gene symbol.

2.2. Differential analysis of GAS5

After upregulation of GAS5 was detected in the plaque group, plaque samples were further stratified into low and high GAS5 groups according to median GAS5 expression. The limma package was used for the differential analysis [22]. Fold changes (FCs) were used to facilitate comparisons between groups. Genes with $|FC|>1.5$ and an adjusted P value < 0.05 were defined as differentially expressed genes (DEGs).

2.3. Enrichment analysis and immune cell evaluation

Genes ordered by FC value were subjected to Gene Set Enrichment analysis (GSEA) for exploring potential biological insights of GAS5 and ANXA2. Reference hallmark gene sets (h.all.v7.5.1.symbols.gmt) were downloaded from the MSigDB database (http://www.gsea-msigdb.org/gsea/downloads.jsp), GSEA was carried out using the R clusterProfiler package [23]. Hallmark terms with absolute normalized enrichment score (NES) greater than 1 and a q value less than 0.05 were retained as statistically significant.

The single-sample GSEA (ssGSEA) algorithm from the R GSVA package was used to evaluate the immune cell enrichment scores

based on a set of metagenes for 28 immune cell subpopulations [24,25]. Different immune cell proportions were assessed using the Immune Cell Abundance Identifier (ImmuCellAI) from the ImmuCellAI package and further validated by CIBERSORTx (https://cibersortx.stanford.edu/) [26,27]. In addition, we examined the associations of mono-macrophage proportions with GAS5 and ANXA2 expression using two other algorithms: MCPcounter and the xCell R package [28,29]. Finally, 122 immunomodulators including chemokines, receptors, major histocompatibility complex molecules, and immune stimulators were analyzed for correlations with GAS5 expression [24]. Correlation between gene expression and different enrichment scores and proportions of immune cells were tested using the Pearson's correlation test.

2.4. Cell culture and treatment

All cell experiments were performed in RAW264.7 macrophages (American Type Culture Collection, Manassas, VA, USA) cultured in Dulbecco's modified Eagle's medium (DMEM, Gibco, Waltham, MA, USA) containing 10 % fetal calf serum (FBS, PAN-Biotech GmbH, Germany) and 1 % penicillin and streptomycin (P/S). Cells were incubated at 37 °C and 5 % CO2 in a humidified incubator. After cultivation overnight, cells were treated with 20 μg/mL ox-LDL (Yiyuan Biotech, Guangzhou, China) for 24 h.

2.5. Cell transfection

Small interfering RNA targeting Gas5 (si-Gas5) and a negative control (si-NC), were purchased from Gene Pharma (Shanghai, China). The sequence of si-Gas5 was 5′-GGCACUGCAAACACAAUGATT-3′, and the sequence of si-NC was 5′-UUCUCCGAACGUGUCACGUTT-3′. Briefly, RAW264.7 cells were seeded into 6-well plates at 1×10^6 cells/well and incubated overnight. When the cells were approximately 50 % confluence, mixtures of Lipofectamine™3000 and Opti-MEM medium (Thermo Fisher Scientific, Waltham, MA, USA), and of siRNA and Opti-MEM medium and were preprepared, separately. The two mixtures were co-incubated for 15 min at room temperature and added to the cells. After transfection at 37 °C for 24 h, the cells were treated with ox-LDL (20 μg/mL) for 24 h. Transfection efficiency was verified by qRT-PCR.

Lentivirus particles carrying short hairpin RNA targeting Gas5(sh-Gas5) and empty vectors (sh-NC) were provided by GenePharma (Shanghai, China). RAW264.7 cells were transfected at a multiplicity of infection (MOI) of 10 in the presence of 15 μg/mL polybrene. The growth medium was replaced 24 h after infection. After 72 h of incubation, the cells were screened with 2.0 μg/mL puromycin and cultured in a humidified incubator (95 % air, 5 % CO2, and 37 °C).

Overexpression plasmids targeting ANXA2 were constructed by Tsingke Biotechnology Co., Ltd., (Beijing, China), and transfected into *Escherichia coli* DH5α receptor cells. The cells were cultured overnight at 37 °C. A Plasmid Extraction Mini Kit (Tsingke Biotechnology, Beijing, China) was used to extract the overexpressed plasmid for subsequent transfection experiments with Lipofectamine™3000. The transfection medium was replaced 4–6 h later with fresh complete culture medium. After 72 h, the proteins were extracted for subsequent Western blot analysis.

2.6. Quantitative reverse-transcription polymerase chain reaction (qRT-PCR)

Total RNA was extracted from cells using TRIzol reagent (Solarbio, Invitrogen, Waltham, MA, USA). cDNA was synthesized from mRNAs using a Fast All-in-One RT Kit (ES Science, China). qRT-PCR was performed using SYBR Green (Thermo Fisher Scientific) and a CFX96 detection system (Bio-Rad, Hercules, CA, USA) to measure gene expression. The relative quantitative 2^{-ddCT} technique was used to measure relative gene expression by adjusting the values to that of the reference gene β-actin (mRNA). The primers used are listed in Table 1.

2.7. Western blot assays

Western blotting was used to detect the expression of related proteins. RIPA lysate and phenylmethylsulfonyl fluoride were used at a 100:1 ratio to prepare cell suspensions. A premade 12 % gel was used in sodium dodecyl sulfate-polyacrylamide gel electrophoresis. The antibodies were then diluted in the following proportions before storing at 4 °C for 12 h: Bax (1:2000; Pro-teintech, Rosemont, IL, USA), Bcl-2 (1:1000; Proteintech), caspase-3 (1:1000; Proteintech), IL-1β(1:1000; Santa, Cruz Biotechnology, Dallas, TX USA), TNF-α (1:1000; Proteintech), and ANXA2 (1:1000; Proteintech). The samples were transferred onto PVDF membranes. After blocking with 5 % skim milk, the membranes were incubated with primary antibodies overnight at 4 °C. The membranes were then incubated with

Table 1
The Sequences of specific primers.

Gene name	Primer sequence (5' to 3')
Gas5	Forward: 5′-GCTCCTGTGACAAGTGGACA-3′, Reverse: 5′-TCTTCTATTTGAGCCTCCATCCA-3′;
Anxa2	Forward: 5′-TGGAGAACGCCTTCCTGAAC-3′, Reverse: CCCTTGGTGTCTTGCTGGAT-3′.
β-actin	Forward: 5′-TGGAATCCTGTGGCATCCATGAAAC-3′, Reverse: 5′-TAAAACGCAGCTCAGTAACAGTCCG-3′;

secondary antibodies for 2 h at room temperature. The signal was acquired using a Bio-Rad Universal Hood II imaging system.

2.8. Animal experiments

Male C57BL/6 J background mice (8–12weeks old) deficient in the gene encoding apolipoprotein-E (ApoE$^{-/-}$) and wild-type controls (C57BL/6 J) were obtained from experimental Animal Center of Tongji University. The ApoE knockout mice were fed a Western-type high-fat, high-cholesterol diet(D12109C, Research Diets, New Jersey, USA) (AS group) for 16 weeks in order to develop atherosclerotic lesions, and these wild-type controls mice were maintained on a standard rodent chow maintained on a standard rodent chow (1010001, Xietong Shengwu) (WT group). Mice were maintained in a carefully controlled environment that included a 12 h light/dark cycle, a constant temperature of 22 ± 2 °C, humidity levels maintained at 55 ± 10 %, noise below 85 dB, and provided with unrestricted access to both food and water. The aortic arch samples were collected for further experiments.

2.9. Statistical analyses

After testing for normality and equal variance, the corresponding statistical analyses were performed. Relevant descriptions are provided in the legends of each figure. The *in vitro* studies were performed at least three times to ensure the stability of individual results, and the data are presented as mean ± standard deviation. Differences between two groups were compared using an unpaired Student's *t*-test or nonparametric Mann-Whitney *U* test according to data normality. Correlation analysis was performed using Pearson's correlation test. *P* value < 0.05 was considered statistical significance. All statistical analyses were performed using R software (R-project.org, version 4.1.2).

3. Results

3.1. GAS5 is upregulated in plaque and associated with inflammatory activation

A flow diagram of our study is shown in Fig. 1. Higher GAS5 expression was observed in the plaque group (n = 195) in the integrated dataset (Fig. 2A). Similarly, upregulation of GAS5 in plaques was observed in both the GTEx and GSE57691 datasets (Supplementary Figs. 1C–D). Receiver operating characteristic curve analysis showed fair predictive value of GAS5 for atherosclerosis in GSE57691 (Supplementary Fig. 1E). The plaque samples were classified into two groups according to GAS5 expression. A total of 341 DEGs, of which 333 were upregulated and 8 downregulated, were identified during differential analysis (Fig. 2B and Supplementary

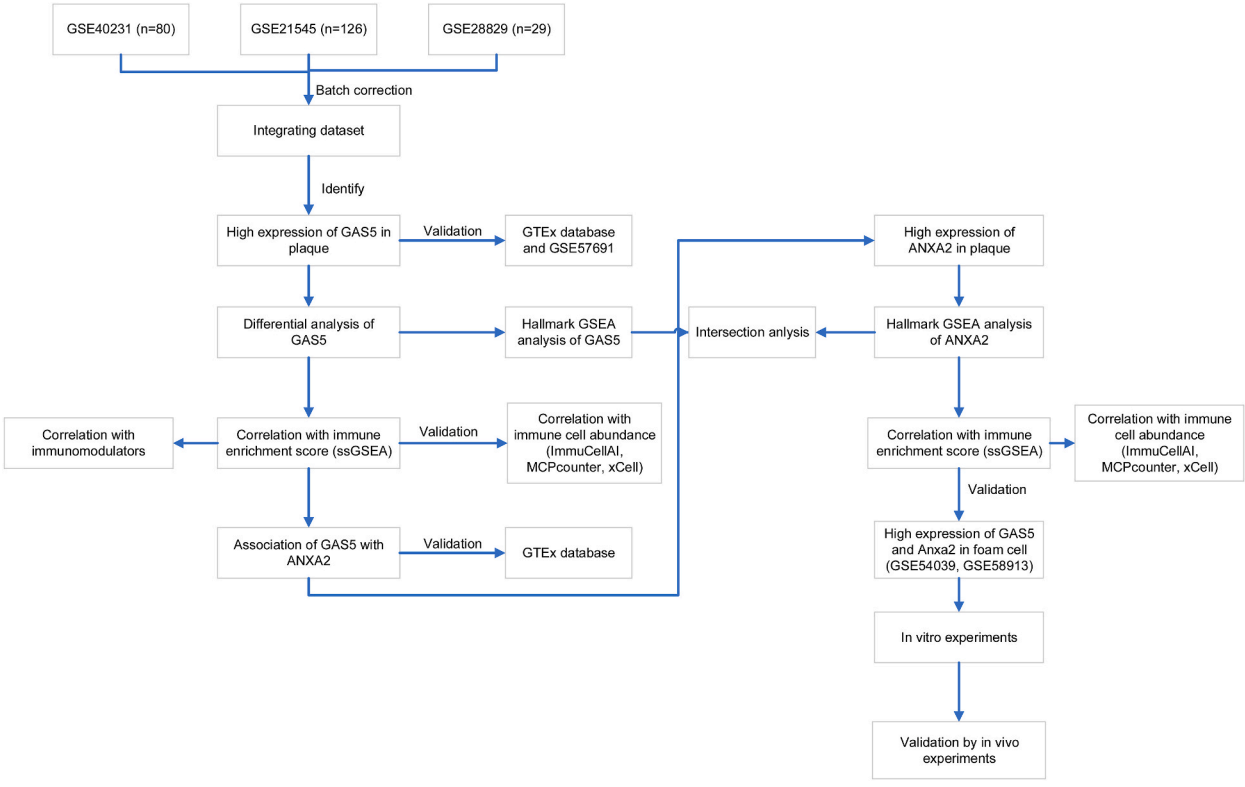

Fig. 1. Flowchart of the study.

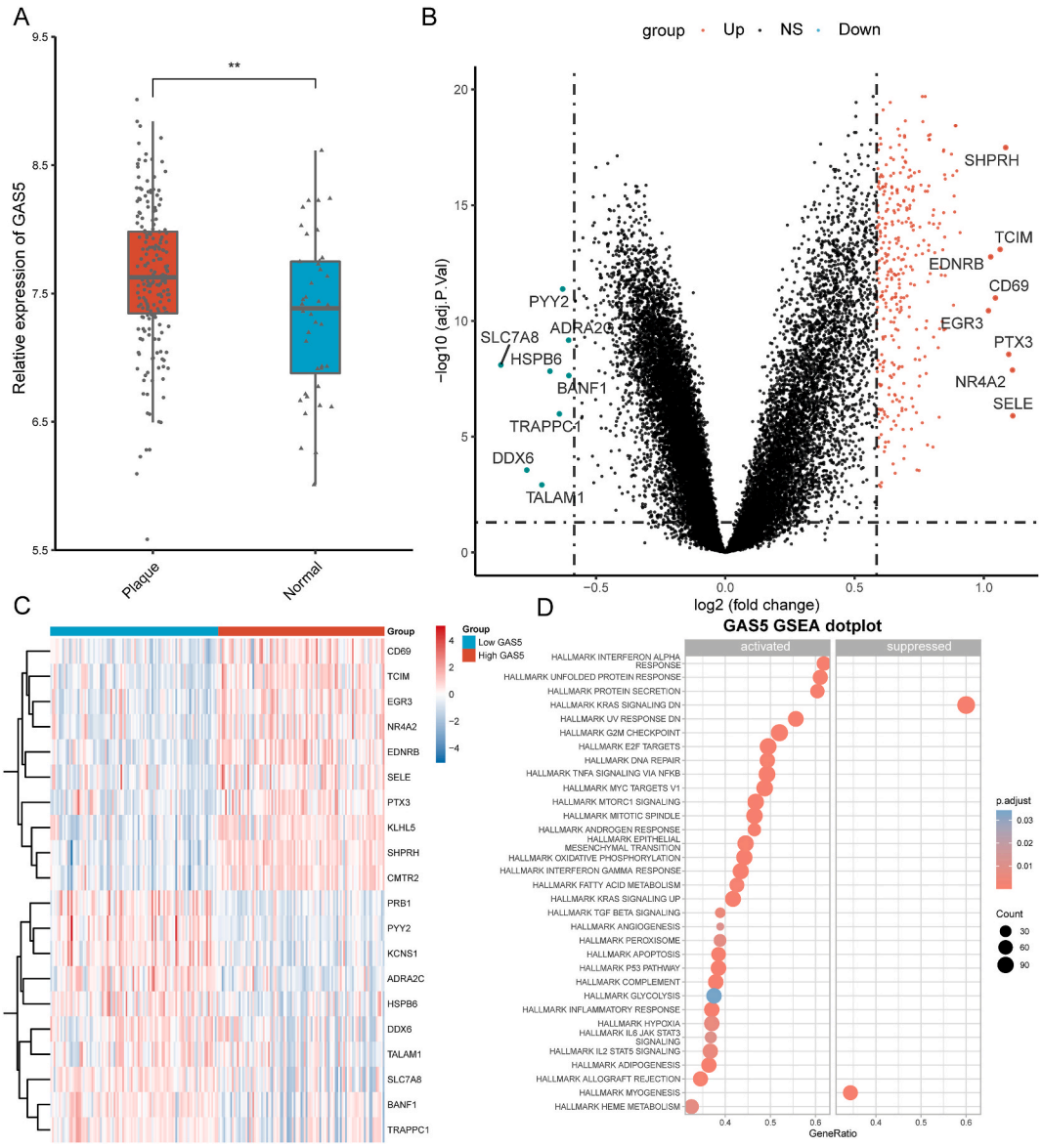

Fig. 2. Differential analysis of GAS5 in the integrated dataset (n = 235). (A) Boxplot of GAS5 expression in plaque (n = 195) and normal tissues (n = 40). (B) Volcano plot of differentially expressed genes that were upregulated in the high (n = 97) and low (n = 98) GAS5 expression groups. (C) Heatmap of the top 10 upregulated and downregulated genes in the high-GAS5 group. (D) Dot plot showing hallmark gene set enrichment analysis (GSEA) of differentially expressed genes in the high-GAS5 group ordered according to fold change value. $^{**}P < 0.01$, as obtained using the Wilcoxon test.

Table 2). The ten most highly upregulated (*CD69, TCIM, EGR3, NR4A2, EDNRB, SELE, PTX3, KLHL5, SHPRH,* and *CMTR2*) and downregulated (*PRB1, PYY2, KCNS1, ADRA2C, HSPB6, DDX6, TALAM1, SLC7A8, BANF1,* and *TRAPPC1*) genes are shown in Fig. 2C. Interestingly, only hallmark terms MYOGENESIS and KRAS_SIGNALING_DN were suppressed, while others (n = 32) were activated in the high GAS5 group (Fig. 2D and Supplementary Table 3). In addition, we performed a differential analysis between the plaque and normal groups in the integrated dataset (Supplementary Table 4). GSEA showed that most signaling pathways upregulated in plaques overlapped with those upregulated the in high GAS5 group, including the hallmark terms INTERFERON_GAMMA_RESPONSE, APOPTOSIS, TNFA_SIGNALING_VIA_NFKB, and INFLAMMATORY_RESPONSE. (Supplementary Figs. 1F–G). These results demonstrated upregulation of GAS5 in plaques and suggested the role of GAS5 in the inflammatory response during atherosclerosis development (e.g. hallmark terms INTERFERON_GAMMA_RESPONSE, TNFA_RESPONSE, APOPTOSIS_PATHWAY).

3.2. GAS5 expression is positively correlated with macrophage activation

First, we performed ssGSEA and CIBERSORTx analyses on the integrated dataset. Macrophages, the main component of immune cells, were activated in the plaque group (Supplementary Figs. 2A–B). Compared to the normal group, GAS5 expression was positively correlated with immune cell proportions and enrichment scores, including for macrophage, gamma delta T cell, and eosinophil. (Fig. 3A and B and Supplementary Fig. 3A). In particular, M1 macrophage, which is associated with the inflammatory macrophage phenotype, was positively associated with GAS5 expression [8]. Furthermore, ImmuCellAI analysis was applied to validate the association between GAS5 expression and the immune response. The estimated immune cell infiltration score was significantly higher in the high-GAS5 group (Fig. 3C). In the high GAS5 group, only macrophages were more abundant (Fig. 3D), suggesting that GAS5 is involved in macrophage activation in atherosclerosis. Furthermore, two other immune estimation algorithms (MCPCounter and xCell) showed higher proportions of monocytic lineages (MCPCounter) and M1 macrophage (xCell) in the high-GAS5 group (Supplementary Fig. 3B). In addition, we found that GAS5 expression correlated with most immunomodulators, especially chemokines (Supplementary Fig. 3C and Supplementary Table 5). Taken together, the five algorithms indicated that GAS5 expression was strongly related to the abundance of macrophage, particularly the M1 subtype.

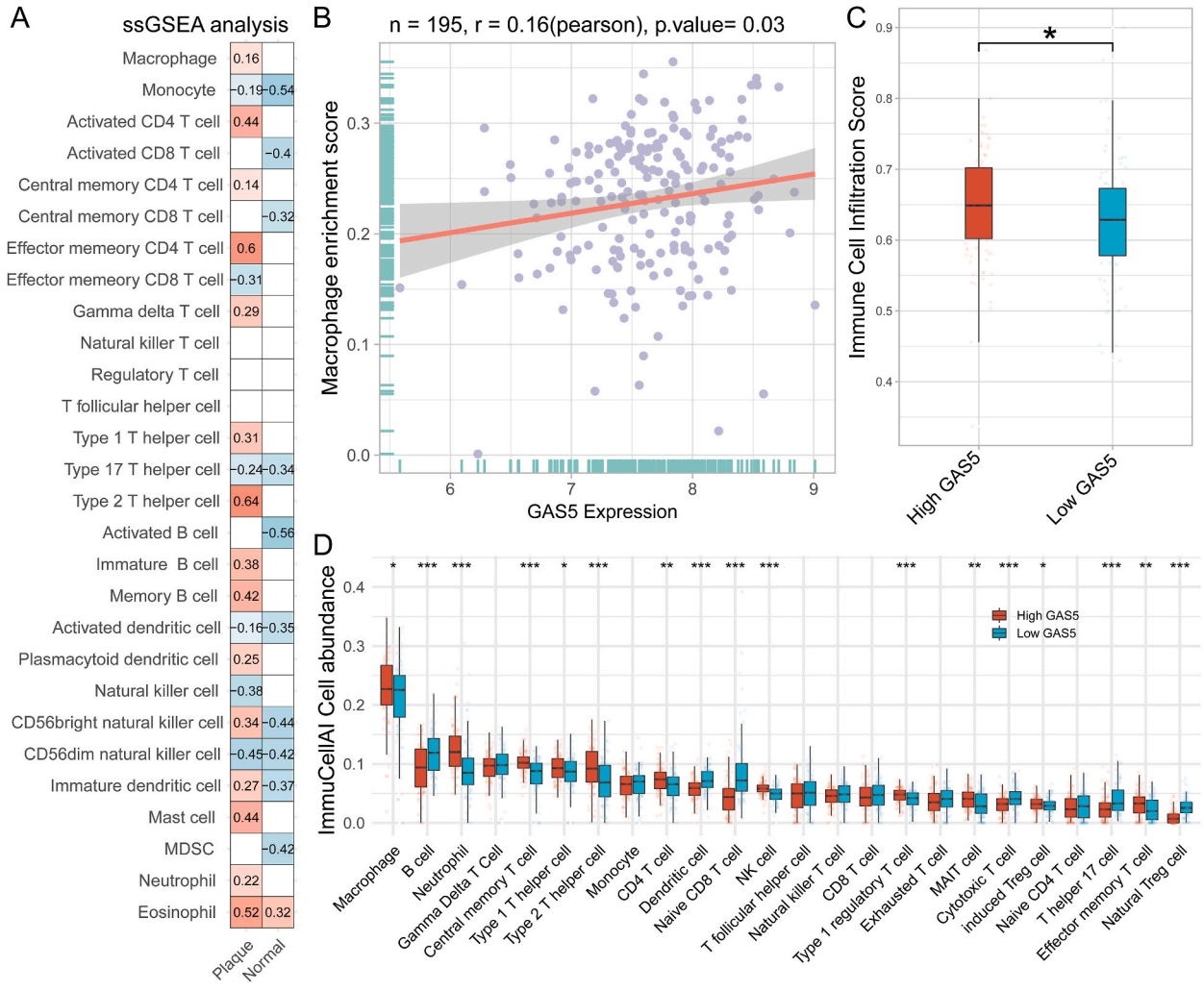

Fig. 3. Association of GAS5 expression with immune infiltration in the integrated dataset. (A) Correlation heatmap of GAS5 expression with 28 immune cell types as determined by ssGSEA of samples divided into normal (n = 40) and plaque (n = 195) groups. (B) Correlation between GAS5 expression and macrophage enrichment score (ImmuCellAI analysis). (C) Boxplot of immune cell infiltration score in high (n = 97) and low (n = 98) GAS5 expression group determined by ImmuCellAI analysis. *$P < 0.05$, as obtained using unpaired Student's *t*-test. (D) Boxplots of relative abundance of 24 immune cell types assessed by ImmuCellAI analysis in the high (n = 97) and low (n = 98) GAS5 expression groups. *$P < 0.05$, **$P < 0.01$, and ***$P < 0.01$ as obtained using the Wilcoxon test.

3.3. Correlation between GAS5 and ANXA2 in plaque

The negative association of GAS5 with ANXA2 expression in normal arterial samples (r = −0.32, $P = 0.04$) was reversed in plaque samples (r = 0.19, $P = 0.01$) (Fig. 4A and B). In addition, expression levels were positively correlated in plaque samples (r = 0.19, $P = 0.02$) in the GTEx dataset, but not in normal samples (r = −0.07, $P = 0.52$) (Supplementary Figs. 4A–B). Differential analysis showed higher ANXA2 expression in the plaque group than in the normal group (Fig. 4C). Furthermore, GSEA of ANXA2 revealed that most hallmark terms (n = 33) were activated with only five suppressed (Fig. 4D and Supplementary Table 6). Intersection analysis was performed to identify biological function similarities between GAS5 and ANXA2. We found that most of the hallmark items overlapped (25 were activated and 1 suppressed; Fig. 4E). Common hallmark terms were associated with upregulated inflammation, apoptosis, and suppressed myogenesis (Fig. 4F and Supplementary Fig. 4C). Accordingly, we hypothesized that ANXA2 is the target of GAS5 during atherosclerosis development and that both are related to the inflammatory response.

3.4. ANXA2 is associated with macrophage activation

The enrichment scores and abundances of different macrophage subtypes and gamma delta T cells were positively associated with ANXA2 expression in the plaque group, as analyzed using both ssGSEA and CIBERSORTX algorithms (Supplementary Figs. 5A–B). Similarly, higher macrophage activity was observed in the high-ANXA2 group (Fig. 5A and B). According to the result of ImmuCellAI, MCPcounter, and xCell analyses, upregulated ANXA2 expression was associated with higher macrophage abundance according to the results (Fig. 5C and Supplementary Figs. 5C–D). Additionally, we identified an increased immune cell infiltration score in the high-

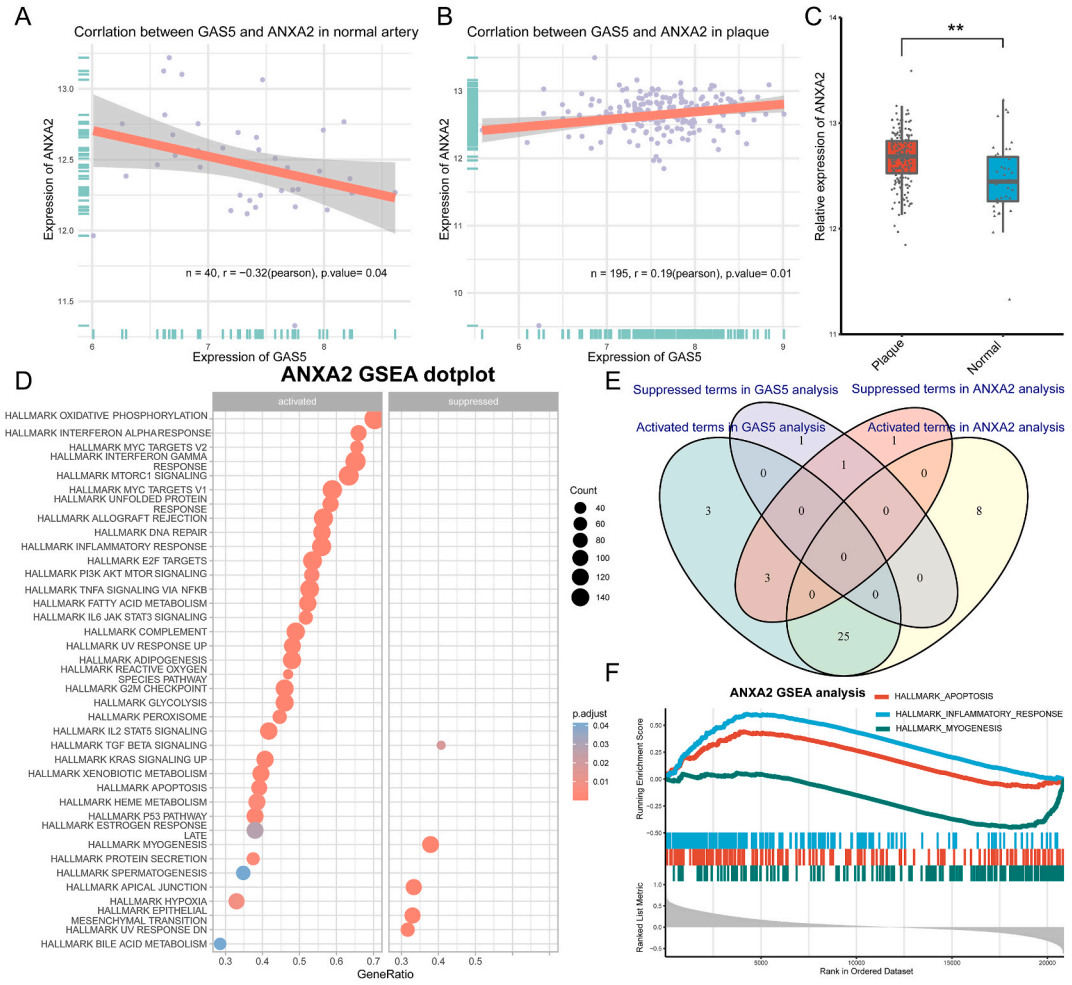

Fig. 4. Positive association of GAS5 with ANXA2 in plaque. The correlation between GAS5 and ANXA2 in (A) normal artery samples (n = 40) and (B) plaque samples (n = 195). (C) Boxplot of ANXA2 expression in plaque (n = 195) and normal tissue (n = 40). (D) Dot plot showing hallmark gene set enrichment analysis (GSEA) of differentially expressed genes in the high-ANXA2 group. (E) Intersection analysis of dysregulated terms from GAS5 and ANXA2 GSEA. (F) The significantly co-enriched hallmark gene sets using GSEA with the immune gene set. **$P < 0.01$, as obtained using the Wilcoxon test.

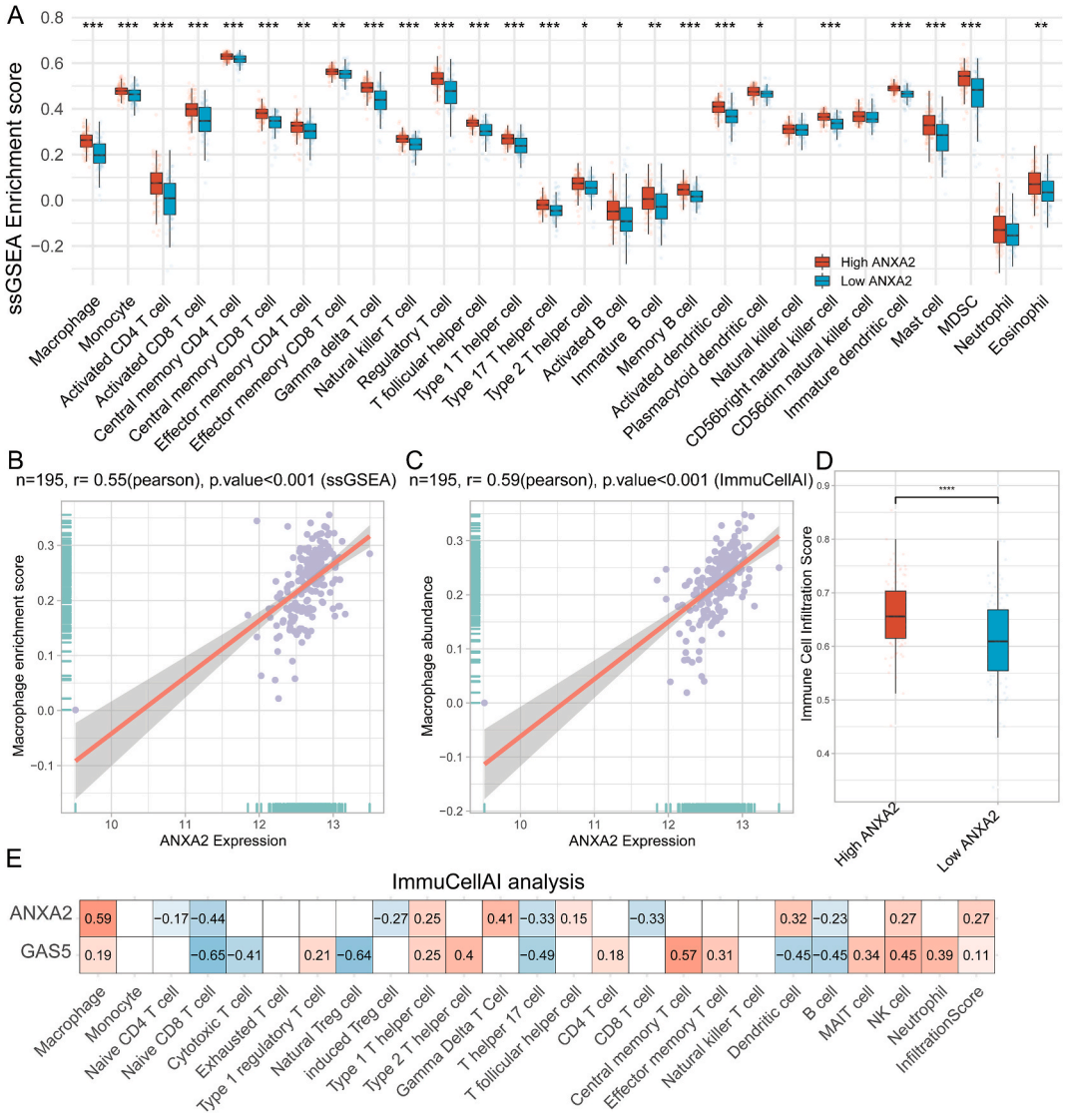

Fig. 5. The association of GAS5 expression with immune infiltration in integrated dataset. (A) Correlation heatmap of ANXA2 with enrichment scores of 28 types of immune cell as determined by ssGSEA of normal (n = 40) and plaque (n = 195) samples. (B) Correlation between ANXA2 expression and macrophage enrichment score as determined by ssGSEA. (C) Correlation between ANXA2 expression and macrophage abundance through ImmuCellAI analysis. (D) Boxplot of immune cell infiltration score in high (n = 97) and low (n = 98) ANXA2 expression group determined by ImmuCellAI analysis. (E) Boxplots of relative abundances of 24 types of immune cell as determined by ImmuCellAI analysis of the high (n = 97) and low (n = 98) ANXA2 expression groups. ****$P < 0.0001$, as obtained using the Wilcoxon test.

ANXA2 group (Fig. 5D). Finally, we examined associations of immune cell types with GAS5 and ANXA2 expression in the plaque group. Expression levels of both GAS5 and ANXA2 are positively correlated with macrophages, type 1 T helper cells, and NK cells (Fig. 5E). Therefore, we hypothesized that both GAS5 and ANXA2 are associated with the macrophage during atherosclerosis development. Data from GSE58913 and GSE54039 were used to examine changes in Anxa2 and Gas5 expression after ox-LDL treatment of macrophages. Anxa2 expression was upregulated in mouse peritoneal macrophages after ox-LDL stimulation (Supplementary Fig. 6A). Furthermore, increased GAS5 expression was observed in THP-1 macrophage-derived foam cells (Supplementary Fig. 6B). In summary, both GAS5 and ANXA2 were correlated with macrophage activation in atherosclerosis.

3.5. Si-Gas5 and Anxa2 overexpression regulates macrophage inflammation

To investigate the function of GAS5 in the macrophage during atherosclerosis development, we downregulated GAS5 in RAW264.7 cells. qRT-PCR showed that GAS5 expression was significantly lower and more stable in cells transfected with Gas5 si-308 compared with cells transfected with Gas5 si-427 or Gas5 si-193 (Supplementary Fig. 6C). Therefore, Gas5 si-308 was selected for subsequent

analyses because of its significant silencing efficiency (henceforth referred to as si-Gas5). qRT-PCR analysis of relative Gas5 and Anxa2 expression revealed that both were upregulated in cells treated with ox-LDL but downregulated following si-Gas5 transfection (Fig. 6A and B). Western blot assays were used to examine changes in cell function after Gas5 knockdown (Fig. 6C). Protein expression of the downstream target Anxa2 showed the same trend as RNA expression (Fig. 6D). Apoptosis markers (Bax, Bcl-2, and caspase-3) and inflammatory molecules (IL-1β and TNF-α) were upregulated in macrophages after ox-LDL treatment but this change was reversed after application of si-Gas5 (Fig. 6E–I).

After silencing Gas5 in ox-LDL-exposed macrophages, decreased Anxa2 expression and functional alterations in the cells were observed. Hence, the regulatory functions of Anxa2 in macrophages treated with ox-LDL were explored using western blotting (Fig. 7A). Anxa2 protein expression increased in ox-LDL-treated macrophages and was further upregulated following transfection with an Anxa2 overexpression plasmid (OE-Anxa2) (Fig. 7B). Furthermore, OE-Anxa2 augmented the levels of apoptosis molecules Bax, Bcl-2, and caspase-3, and pro-inflammatory proteins IL-1β and TNF-α following ox-LDL stimulation (Fig. 7C–G). These results suggested that both Gas5 and Anxa2 regulated the inflammatory response of macrophages under ox-LDL treatment.

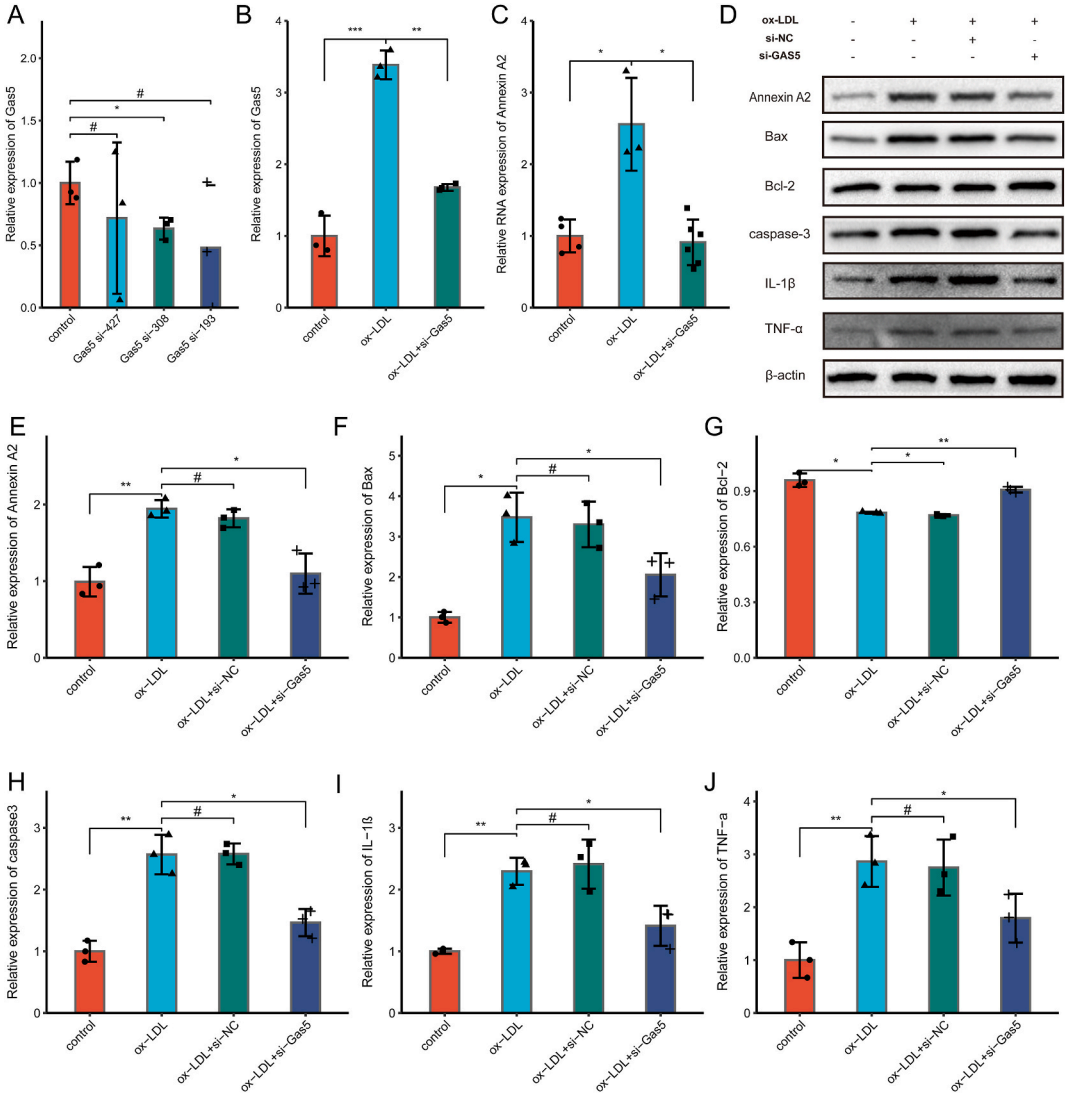

Fig. 6. GAS5 regulated macrophage apoptosis and inflammation *in vitro*The expression levels of (A) Gas5 and (B) Anxa2 were upregulated in the ox-LDL-treated group and downregulated when incubated with a small interfering RNA Gas5 (si-Gas5). (C) Western blotting assays analyzing the effect of Gas5 on apoptosis (Bax, Bcl-2, caspase-3) and inflammation (IL-1β and TNF-α levels) in RAW264.7 cells. Changes in expression levels of (D) Anxa2, (E) Bax, (F) Bcl-2, (G) caspase-3, (H) IL-1β, and (I) TNF-α in ox-LDL-treated RAW264.7 cells after si-Gas5 treatment. Data are presented as mean ± standard error of the mean (SEM) of at least three independent experiments. $^{\#}P > 0.05$, $^{*}P < 0.05$, $^{**}P < 0.01$, and $^{***}P < 0.001$. For two groups, data were compared using the Mann-Whitney *U* test.

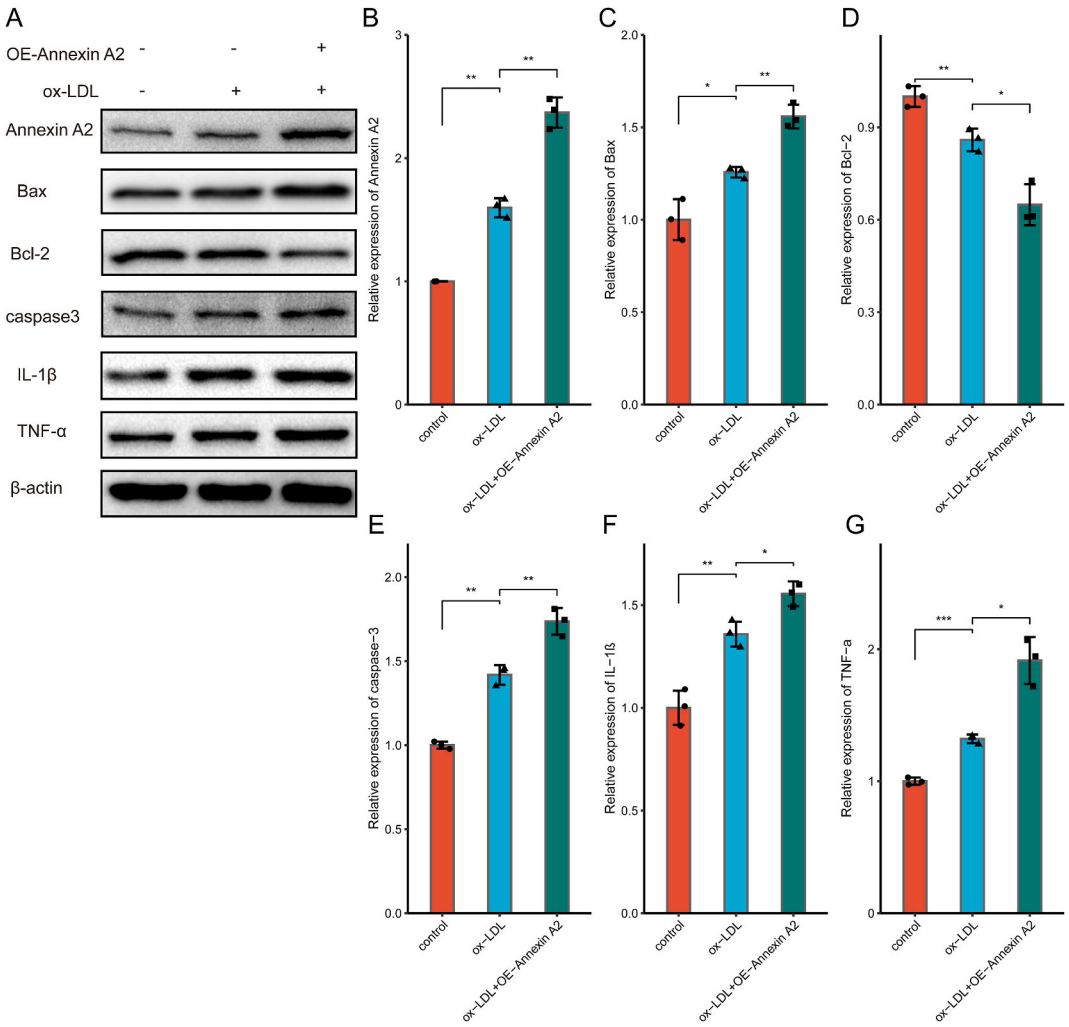

Fig. 7. ANXA2 regulated macrophage apoptosis and inflammation *in vitro*. (A) Western blotting analyzing the effect of an annexin A2-overexpressing plasmid (OE-Annexin A2) on ANXA2, apoptosis (Bax, Bcl-2, and caspase-3), and inflammation (IL-1β, TNF-α) in RAW264.7 cells. The expression levels of (B) Anxa2, (C) Bax, (D) Bcl-2, (E) caspase-3, (F) IL-1β, and (G) TNF-α in OE-Annexin A2 and ox-LDL-treated RAW264.7 cells. Data are presented as mean ± SEM of at least three independent experiments. $^{*}P < 0.05$, $^{**}P < 0.01$, and $^{***}P < 0.001$. For two groups, data were compared using the Mann-Whitney *U* test.

3.6. Macrophage inflammatory response is regulated by the GAS5-ANXA2 axis

To elucidate the effect of the GAS5-ANXA2 axis on macrophages, we simultaneously adjusted Gas5 and Anxa2 expression using Gas5 shRNA and OE-Anxa. RT-qPCR showed that Gas5 expression decreased after sh-Gas5 treatment, indicating efficient transfection (Fig. 8A). Western blotting revealed that the pro-inflammatory function of GAS5 was Anxa2-dependent (Fig. 8B). Anxa2 protein expression was downregulated by sh-GAS5 and upregulated by OE-Anxa2 (Fig. 8C). Apoptosis (as indicated by Bax, Bcl-2, and caspase-3 levels) and inflammation (by IL-1β and TNF-α levels) in ox-LDL-treated macrophage were inhibited by sh-Gas5 and this change was reversed following OE-Anxa2 transfection (Fig. 8D–H). This result indicated the regulatory role of Gas5 in the macrophage inflammatory response is dependent on Anxa2.

3.7. Differential expression of Gas5 and Anxa2 in plaque through in vivo experiments

To validate the upregulation of Gas5 and Anxa2 during atherosclerosis development, the aorta arch samples from WT and AS group were collected. We observed significant increase of Gas5 in AS group (Fig. 9A). Consistently, ANXA2 is upregulated in AS group, compared with WT group (Fig. 9B).

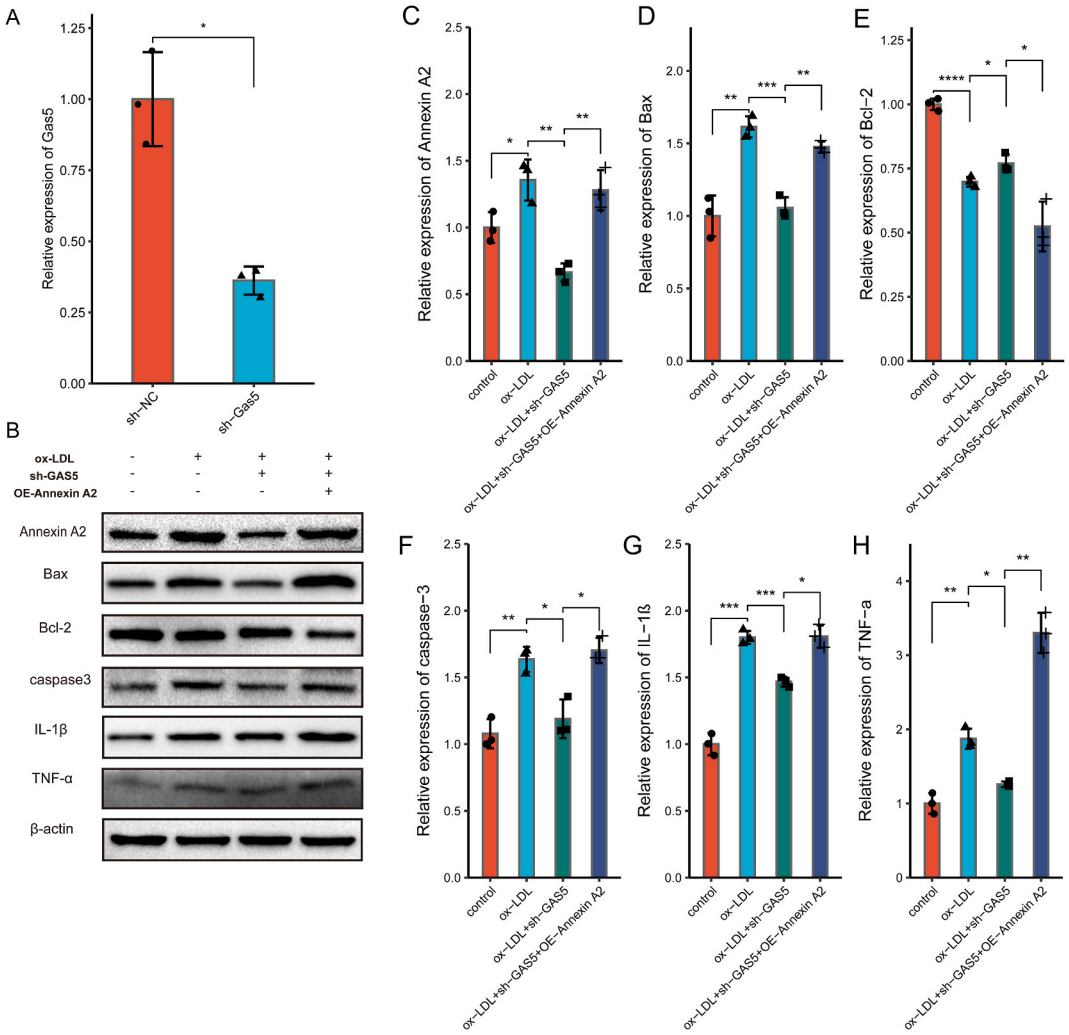

Fig. 8. The GAS5-ANXA2 axis contributed to the apoptosis and inflammation of macrophages. (A) The knockdown efficiency of a short hairpin RNA targeting (sh-Gas5) on Gas5 in RAW264.7 cells. (B) Western blotting illustrated the effect of sh-Gas5 and sh-Gas5+OE-Annexin A2 on ANXA2, apoptosis (Bax, Bcl-2, caspase-3), and inflammation (IL-1β, TNF-α) in RAW264.7 cells. Changes in expression levels of (C) Anxa2, (D) Bax, (E) Bcl-2, (F) caspase-3, (G) IL-1β, and (H) TNF-α in ox-LDL-treated RAW264.7 cells treated with sh-Gas5, and by OE-Annexin A2. Data are presented as mean ± SEM of at least three independent experiments. *P < 0.05, **$P < 0.01$, and ***$P < 0.001$. For two groups, data were compared using the Mann-Whitney U test.

4. Discussion

Through bioinformatics analysis, we found that both GAS5 and ANXA2 are involved in atherosclerosis development and macrophage activation. *In vitro* experiments showed that the GAS5-ANXA2 axis regulated the inflammatory response of macrophages following ox-LDL treatment.

Macrophages, which can be divided into tissue-resident and monocyte-derived, play key roles in atherogenesis and progression [30]. Depending on stimuli, macrophages transition toward either the inflammatory (also recognized as M1) or TREM2 (also recognized as M2) phenotype [31,32]. Inflammatory macrophages, which are enriched in cytokines (such as IL1α, IL1β, and TNF) and chemokines (such as CXCL2, CXCL1, CCL3, CCL4, and CXCL10), induce atherogenesis by regulating functional alterations in endothelial cells, phenotypic switches in smooth muscle cells, imbalances of effector and regulatory T cells, and extracellular matrix remodeling [30,33–35]. In the present study, we identified that both GAS5 and ANXA2 participated in the immune response. Although expression levels of both GAS5 and ANXA2 correlated with different T cell subtypes (such as activated CD4, central memory CD8, and effector memory CD4 T cells), these associations were not consistent across the three algorithms (CIBERSORTx, xCell, and MCPCounter) (Supplementary Figs. 3A and 7). Only the activation of macrophages in plaques were correlated with GAS5 and ANXA2 expression. Interestingly, CIBERSORTx analysis showed that GAS5 and ANXA2 expression levels were significantly correlated with M1but not M2 macrophages, indicating that the GAS5-ANXA2 axis may play a critical role in the macrophage inflammatory response.

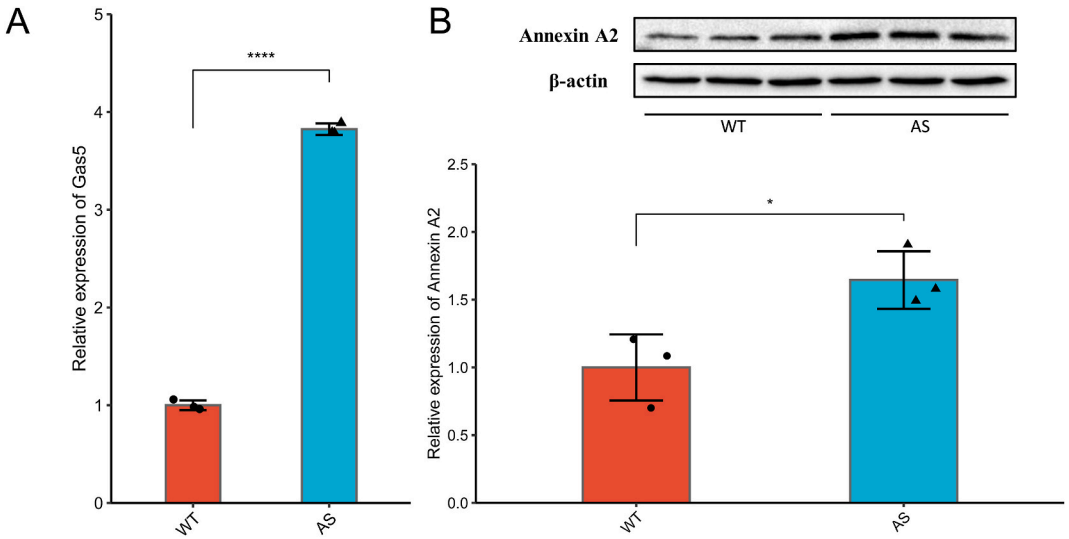

Fig. 9. In vivo experiments identify the differentially expressed GAS5 and ANXA2 in aorta of mice. (A) qRT-PCR indicates the upregulated Gas5 expression in atherosclerosis (AS) group. (B) Western blot assays show that ANXA2 is upregulated in AS group. Data are presented as mean ± SEM of at least three independent experiments. Significance is indicated as follows: *P < 0.05, **$P < 0.01$, and ***$P < 0.001$. For two groups, data were compared using the Mann-Whitney U test.

Previous studies have revealed the potential atherogenic role of GAS5 through its upregulation in endothelial cells and macrophages following ox-LDL stimulation [13,36]. GAS5 knockdown suppressed apoptosis, inflammation, and cholesterol efflux in ox-LDL treated THP-1 cells [16,17,37,38]. A study of 98 patients with coronary heart disease revealed that circulating GAS5 was associated with decreased high-density lipoprotein cholesterol and increased C-reactive protein and Gensini scores [39]. However, the potential relationship between GAS5 and macrophages in plaques is unclear. Hence, we explored the association of GAS5 with inflammatory macrophages in human plaque samples and validated a new regulatory mechanism for GAS5 in mouse macrophages.

ANXA2, a member of the conserved annexin X family, is a calcium-regulated phospholipid-binding protein [40–42]. ANXA2 exists in the cytoplasm and cell membranes and is presents in different cell lines, including endothelial cells, macrophages, and tumor cells [43]. Monomers and heterotetramers of ANXA2, which are composed of two copies of ANXA2 monomers and two copies of S100A10, activate fibrinolysis, and inhibit PCSK9 levels and cholesterol accumulation [44–46]. Zhang et al. found that ANXA2 deficiency suppressed endothelial cell activation and atherosclerosis development in regions with disturbed blood flow in mice [47]. However, the association between ANXA2, macrophage, and atherosclerosis in human datasets has not yet been elucidated. In the present study, we identified a significant correlation between ANXA2 expression and atherosclerosis in a large cohort. Furthermore, we found that Anxa2 regulated the inflammatory response of ox-LDL-treated macrophages using both bioinformatic and *in vitro* analyses.

In conclusion, the atherogenic roles of GAS5 and ANXA2 in the inflammatory response of macrophages (inflammation and apoptosis) was identified. We found that ANXA2 is a novel target of GAS5 in macrophages during atherosclerosis development. We have provided a new perspective on macrophage inflammation and GAS5 using multiple large datasets and several immune analysis algorithms. Additionally, our analysis identified a new GAS5 target, and described the association of ANXA2 with atherosclerosis and macrophage inflammatory responses. Furthermore, *in vivo* experiments help validate differences between GAS5 and ANXA2 expression in plaque and normal groups.

Data availability statement

The data that support the findings of this study are publicly available in the GEO (GSE40231, GSE21545, and GSE28829) and GTEx database. The expression matrix and custom scripts in this study and corresponding codes are available on request from the corresponding author.

Ethics declaration

Animal experimental procedures were conducted in compliance accordance with ethical standards and received prior approval from the Ethics Committee of Shanghai Tenth People's Hospital (SHDSYY-2023-4987). All experimental procedures were performed in accordance with the National Institute of Health Guide for the Care and Use of Laboratory Animals.

CRediT authorship contribution statement

Yuzhou Xue: Visualization, Validation, Software, Data curation. **Yu Hu:** Validation, Data curation. **Shikai Yu:** Investigation, Data

curation. **Wenyan Zhu:** Validation, Data curation. **Lin Liu:** Visualization, Software. **Minghao Luo:** Data curation. **Suxin Luo:** Writing – original draft, Conceptualization. **Jian Shen:** Writing – original draft. **Longxiang Huang:** Writing – review & editing. **Jie Liu:** Validation. **Dingyi Lv:** Visualization. **Wenming Zhang:** Validation. **Jingyu Wang:** Data curation. **Xiang Li:** Writing – review & editing, Writing – original draft, Conceptualization.

Declaration of competing interest

The authors declare that they have no known competing financial interests or personal relationships that could have appeared to influence the work reported in this paper.

Acknowledgements

The study was supported by the General Project of Chongqing Natural Science Foundation (project number: cstc2020jcyj-msxmX1091), and Intelligent Medicine Training Program of Chongqing Medical University (project number: ZHYX202017). The language editing of this study was performed by Editage.

Appendix A. Supplementary data

Supplementary data to this article can be found online at https://doi.org/10.1016/j.heliyon.2024.e24103.

References

[1] X. Du, et al., Epidemiology of cardiovascular disease in China and Opportunities for improvement: JACC international, J. Am. Coll. Cardiol. 73 (24) (2019) 3135–3147.
[2] G.A. Roth, et al., Global burden of cardiovascular diseases and risk factors, 1990-2019: update from the GBD 2019 study, J. Am. Coll. Cardiol. 76 (25) (2020) 2982–3021.
[3] I. Tabas, A.H. Lichtman, Monocyte-Macrophages and T Cells in atherosclerosis, Immunity 47 (4) (2017) 621–634.
[4] K.J. Moore, et al., Macrophage trafficking, inflammatory resolution, and genomics in atherosclerosis: JACC macrophage in CVD series (Part 2), J. Am. Coll. Cardiol. 72 (18) (2018) 2181–2197.
[5] H. Winkels, et al., Atlas of the immune cell repertoire in mouse atherosclerosis defined by single-cell RNA-sequencing and mass cytometry, Circ. Res. 122 (12) (2018) 1675–1688.
[6] D.M. Fernandez, et al., Single-cell immune landscape of human atherosclerotic plaques, Nat. Med. 25 (10) (2019) 1576–1588.
[7] A. Zernecke, et al., Meta-analysis of leukocyte diversity in atherosclerotic mouse aortas, Circ. Res. 127 (3) (2020) 402–426.
[8] L. Willemsen, M.P. de Winther, Macrophage subsets in atherosclerosis as defined by single-cell technologies, J. Pathol. 250 (5) (2020) 705–714.
[9] K. Kim, et al., Transcriptome analysis reveals nonfoamy rather than foamy plaque macrophages are proinflammatory in atherosclerotic murine models, Circ. Res. 123 (10) (2018) 1127–1142.
[10] J.D. Lin, et al., Single-cell analysis of fate-mapped macrophages reveals heterogeneity, including stem-like properties, during atherosclerosis progression and regression, JCI Insight 4 (4) (2019).
[11] J.B. Pierce, M.W. Feinberg, Long noncoding RNAs in atherosclerosis and vascular injury: pathobiology, biomarkers, and targets for therapy, Arterioscler. Thromb. Vasc. Biol. 40 (9) (2020) 2002–2017.
[12] Z. Zhang, D. Salisbury, T. Sallam, Long noncoding RNAs in atherosclerosis: JACC review topic of the week, J. Am. Coll. Cardiol. 72 (19) (2018) 2380–2390.
[13] Y. Yan, et al., Long non-coding RNAs link oxidized low-density lipoprotein with the inflammatory response of macrophages in atherogenesis, Front. Immunol. 11 (2020) 24.
[14] Y. Ding, et al., The combined regulation of long non-coding RNA and RNA-binding proteins in atherosclerosis, Front. Cardiovasc. Med. 8 (2021) 731958.
[15] S. Zhang, et al., Recent advances in the regulation of ABCA1 and ABCG1 by lncRNAs, Clin. Chim. Acta 516 (2021) 100–110.
[16] Y. Zhang, et al., GAS5 knockdown suppresses inflammation and oxidative stress induced by oxidized low-density lipoprotein in macrophages by sponging miR-135a, Mol. Cell. Biochem. 476 (2) (2021) 949–957.
[17] S. Shen, et al., Silencing of GAS5 represses the malignant progression of atherosclerosis through upregulation of miR-135a, Biomed. Pharmacother. 118 (2019) 109302.
[18] J. Ye, et al., LncRBA GSA5, up-regulated by ox-LDL, aggravates inflammatory response and MMP expression in THP-1 macrophages by acting like a sponge for miR-221, Exp. Cell Res. 369 (2) (2018) 348–355.
[19] L. Li, et al., Low expression of lncRNA-GAS5 is implicated in human primary varicose great saphenous veins, PLoS One 10 (3) (2015) e0120550.
[20] L. Gautier, et al., affy–analysis of Affymetrix GeneChip data at the probe level, Bioinformatics 20 (3) (2004) 307–315.
[21] J.T. Leek, et al., The sva package for removing batch effects and other unwanted variation in high-throughput experiments, Bioinformatics 28 (6) (2012) 882–883.
[22] M.E. Ritchie, et al., Limma powers differential expression analyses for RNA-sequencing and microarray studies, Nucleic Acids Res. 43 (7) (2015) e47.
[23] G. Yu, et al., clusterProfiler: an R package for comparing biological themes among gene clusters, OMICS 16 (5) (2012) 284–287.
[24] P. Charoentong, et al., Pan-cancer immunogenomic analyses reveal genotype-immunophenotype relationships and predictors of response to checkpoint blockade, Cell Rep. 18 (1) (2017) 248–262.
[25] S. Hänzelmann, R. Castelo, J. Guinney, GSVA: gene set variation analysis for microarray and RNA-seq data, BMC Bioinf. 14 (2013) 7.
[26] Y.R. Miao, et al., ImmuCellAI: a unique method for comprehensive T-cell subsets abundance prediction and its application in cancer immunotherapy, Adv. Sci. 7 (7) (2020) 1902880.
[27] A.M. Newman, et al., Determining cell type abundance and expression from bulk tissues with digital cytometry, Nat. Biotechnol. 37 (7) (2019) 773–782.
[28] D. Aran, Z. Hu, A.J. Butte, xCell: digitally portraying the tissue cellular heterogeneity landscape, Genome Biol. 18 (1) (2017) 220.
[29] E. Becht, et al., Estimating the population abundance of tissue-infiltrating immune and stromal cell populations using gene expression, Genome Biol. 17 (1) (2016) 218.
[30] L.I. Susser, K.J. Rayner, Through the layers: how macrophages drive atherosclerosis across the vessel wall, J. Clin. Invest. 132 (9) (2022).
[31] Z. Hu, et al., Single-cell transcriptomic atlas of different human cardiac arteries identifies cell types associated with vascular physiology, Arterioscler. Thromb. Vasc. Biol. 41 (4) (2021) 1408–1427.

[32] K. Rahman, et al., Inflammatory Ly6Chi monocytes and their conversion to M2 macrophages drive atherosclerosis regression, J. Clin. Invest. 127 (8) (2017) 2904–2915.
[33] M. Song, et al., Crosstalk between macrophage and T cell in atherosclerosis: potential therapeutic targets for cardiovascular diseases, Clin. Immunol. 202 (2019) 11–17.
[34] A. Yurdagul Jr., Crosstalk between macrophages and vascular smooth muscle cells in atherosclerotic plaque stability, Arterioscler. Thromb. Vasc. Biol. 42 (4) (2022) 372–380.
[35] Y. Xue, et al., Macrophages regulate vascular smooth muscle cell function during atherosclerosis progression through IL-1β/STAT3 signaling, Commun. Biol. 5 (1) (2022) 1316.
[36] X. Ma, H. Liu, F. Chen, Functioning of long noncoding RNAs expressed in macrophage in the development of atherosclerosis, Front. Pharmacol. 11 (2020) 567582.
[37] L. Chen, et al., Exosomal lncRNA GAS5 regulates the apoptosis of macrophages and vascular endothelial cells in atherosclerosis, PLoS One 12 (9) (2017) e0185406.
[38] X.D. Meng, et al., Knockdown of GAS5 inhibits atherosclerosis progression via reducing EZH2-mediated ABCA1 transcription in ApoE(-/-) mice, Mol. Ther. Nucleic Acids 19 (2020) 84–96.
[39] Y. Jiang, T. Du, Relation of circulating lncRNA GAS5 and miR-21 with biochemical indexes, stenosis severity, and inflammatory cytokines in coronary heart disease patients, J. Clin. Lab. Anal. 36 (2) (2022) e24202.
[40] V. Gerke, S.E. Moss, Annexins: from structure to function, Physiol. Rev. 82 (2) (2002) 331–371.
[41] V. Gerke, C.E. Creutz, S.E. Moss, Annexins: linking Ca2+ signalling to membrane dynamics, Nat. Rev. Mol. Cell Biol. 6 (6) (2005) 449–461.
[42] Y.Z. Li, et al., Annexin A protein family in atherosclerosis, Clin. Chim. Acta 531 (2022) 406–417.
[43] K.A. Hajjar, J.S. Menell, Annexin II: a novel mediator of cell surface plasmin generation, Ann. N. Y. Acad. Sci. 811 (1997) 337–349.
[44] Q. Li, et al., Plasmin induces intercellular adhesion molecule 1 expression in human endothelial cells via nuclear factor-κB/mitogen-activated protein kinases-dependent pathways, Exp. Biol. Med. 238 (2) (2013) 176–186.
[45] R.H. Fairoozy, et al., Identifying low density lipoprotein cholesterol associated variants in the Annexin A2 (ANXA2) gene, Atherosclerosis 261 (2017) 60–68.
[46] G. Mayer, S. Poirier, N.G. Seidah, Annexin A2 is a C-terminal PCSK9-binding protein that regulates endogenous low density lipoprotein receptor levels, J. Biol. Chem. 283 (46) (2008) 31791–31801.
[47] J.W. Lee, et al., Transcription-independent induction of ERBB1 through hypoxia-inducible factor 2A provides cardioprotection during ischemia and reperfusion, Anesthesiology 132 (4) (2020) 763–780.